Available online at www.sciencedirect.com
SCIENCE DIRECT®
Journal of Nuclear Materials 354 (2006) 28–35
journal of nuclear materials
www.elsevier.com/locate/jnucmat

# Displacement cascade initiated with the realistic energy of the recoil nucleus in $UO_2$ matrix by molecular dynamics simulation

L. Van Brutzel *, M. Rarivomanantsoa, D. Ghaleb

*Commissariat à l'Énergie Atomique, CEA/DEN-DTCD-SECM-LCLT, CEA-Marcoule B.P. 17171, Bagnols sur cèze cedex 30207, France*

Received 11 March 2005; accepted 24 January 2006

**Abstract**

Classical molecular dynamics simulations have been performed to study the primary damage due to α-decay self-radiation in $UO_2$ matrix. For the first time a displacement cascade initiated with an energy of 80 keV has been performed. Compared with the cascades initiated with lower energies of the primary knock-on atom (PKA), the morphology of the cascade shows the same features; no amorphisation and creation of point defects are observed. The discrepancy with the linear theory NRT (Norton–Robinson–Torrens) law on the creation of the number of point defects is discussed. However, differences have been found; local and temporary amorphisation appears during the thermal spike over large length scale only in the high energy cascade. Proportionally in the high energy cascade, more linear collision sequences are undergone by the uranium atoms and the oxygen atoms recombine over a larger length scale.


*PACS:* 61.72.Ji; 61.803.Az; 61.80.Lj

## 1. Introduction

During the storage of spent nuclear fuel, several self-radiation processes could deteriorate the physical and the chemical integrity of the material. Previously, it has been proved that during the first few picoseconds (ps) of an α-decay numerous point defects occur, while the β- and γ-decays release their energy through electronic effects [1,2]. The point defects caused by α-decay move, heal, and/or aggregate forming larger (length scale) defects such as dislocations, bubbles, or stacking faults which affect the structural and the mechanical properties of the material. The study of the primary damage state (point defects caused be an α-decay) is then essential to understand how the material ages. Molecular dynamics (MD) simulations have already successfully modeled this phenomenon in various materials such as metals [3], ceramics [4,5] and glasses [6,7] used in nuclear science applications.

Previous work on uranium dioxide ($UO_2$) has enhanced our understanding of this primary damage state [8] and is in agreement with existing experiments [1,9–13]. Nevertheless, the computational

* Corresponding author. Tel.: +33 4 66 39 79 40; fax: +33 4 66 79 66 20.
*E-mail address:* laurent.vanbrutzel@cea.fr (L. Van Brutzel).

0022-3115/$ - see front matter © 2006 Elsevier B.V. All rights reserved.
doi:10.1016/j.jnucmat.2006.01.020

power limitations have restricted these studies to small displacement cascades which reach only 25% of the real energy of the recoil nucleus. For the first time a displacement cascade initiated at 80 keV, corresponding to a realistic energy of the recoil nucleus during an α-decay, is report herein.

This article is organized as follows. Section 2 presents a brief description of the methods used to simulate the displacement cascade. Section 3 discusses the results of these simulations along with highlighting the differences with the previous works [8] which have been carried out at lower energy of the Primary Knock-on Atom (PKA). Finally, conclusions are stated in Section 4.

## 2. Simulation method

An interatomic potential was previously developed to study the atomic interactions and displacements cascades in $UO_2$ [14]. As pointed out by Becquart et al. [15] the threshold displacement and migration energies of point defects play a critical role in the displacement cascades computed by MD simulations. Therefore, the potential was developed in order to have a reasonable agreement with the formation and migration energies calculated by ab initio simulations [16] and experimental results [17]. It also agrees with the structural properties of the crystal. It is composed of a Born–Mayer–Huggins (BMH) like term, a Van der Waals term and a Coulomb term. The analytical functional defining this potential is

$$V_{\alpha\beta}(r_{ij}) = A_{\alpha\beta}\exp\left(-\frac{r_{ij}}{B_{\alpha\beta}}\right) - \frac{C_{\alpha\beta}}{r_{ij}} + \frac{z_\alpha z_\beta}{4\pi\epsilon_0 r_{ij}},$$

where $A$, $B$ and $C$ are adjustable parameters, $r_{ij}$ is the distance between atom and $z$ is the ionic partial charge. Parameters of the interatomic potential are given in Table 1.

Note that the BMH term of the U–U interaction is assumed to be zero because of the predominance of the electrostatic repulsion and the large distance (3.9 Å at the equilibrium) between two uranium atoms. Also, the Van der Waals terms for the U–U and the U–O interaction are assumed to be zero because of the predominance of the electrostatic component.

Table 1
Parameters of the interatomic potential

| | Z | | $A$ (eV) | $B$ (Å) | $C$ (eV Å$^6$) |
|---|---|---|---|---|---|
| U | +3.22725 | U–U | 0.0 | N/A | 0.0 |
| O | −1.61362 | U–O | 566.498 | 0.42056 | 0.0 |
| | | O–O | 11272.6 | 0.1363 | 134 |

Note that the Born–Mayer–Huggins interaction between U–U atoms is set to zero. The Van der Waals interactions between the U–U atoms and the U–O atoms are also set to zero.

Because of the strong ionic feature of uranium dioxide, a correct description of the coulomb interactions is necessary. Therefore, a complete Ewald summation [18] is computed with a cut-off of 11 Å in the real space and $\pm 6 \times \pm 6 \times \pm 6$ vectors in the reciprocal space.

When the distance between the atoms is approximately the equilibrium distance, the BMH like repulsive potential is a reliable representation of the interaction between the two atoms. However, during the displacement cascades, ballistic shocks cause the interatomic distances to be shorter than their equilibrium distances. For small interatomic distances lower than 1.6 Å, the universal Ziegler–Biersack–Littmark (ZBL) potential is added [19]. The continuity of the overlap between the BMH and the ZBL potentials is achieved with a fifth degree polynomial function chosen so the potential energy, the forces, and the first derivative of the forces are continuous.

Periodic boundary conditions are used to prevent from surface effects. However, the simulation box needs to be large enough to prevent self-interaction of cascades. Therefore, the simulation box was estimated to $68 \times 68 \times 68$ unit cells of the fluorite lattice like $UO_2$ which corresponds to a total of 3 773 184 atoms and a cubic box length of 372 Å. At the end of the simulation we verify that no self-interaction have occurred.

The initial velocities of the atoms are set with a Maxwellian distribution and the average kinetic energy corresponds to a temperature of 300 K. The displacement cascades are initiated by choosing an uranium atom and accelerating it to the corresponding recoil nucleus kinetic energy. This uranium atom represents the effects of the Primary Knock-on Atom (PKA) on the $UO_2$ matrix. Its initial kinetic energy is gradually transferred to other particles of the system through ballistic collisions, which causes the global temperature to increase. This phenomenon is known as the thermal spike. In a rigorous way, the equipartition theorem indicates that half the PKA energy will be released into thermal activity at the equilibrium. In order to maintain a constant temperature during the simulation the velocities of the atoms contained in a 3 Å layer width around the simulation box are

maintained at a temperature equal to 300 K. Every ten time steps the average temperature of this external layer is computed and the velocities of the atoms are rescaled to keep the temperature in this boundary layer equal to 300 K. This technique enables us to extract the kinetic energy at the edges of the box and prevents the interaction between heat wave emitted by the cascade. To reduce the computational time of the simulation during the displacement cascade a variable time step algorithm described in reference [7] is used.

Results presented in the following sections often refer to atoms which are displaced by more than 2 Å. This distance has been chosen based on the analysis of the distance traveled by the atoms. Fig. 1 depicts the total number of atoms versus their displacement from their initial positions during the thermal spike, where the kinetic temperatures are the highest and at the end of the cascade. At the end of the cascade the kinetic temperature is homogeneous and a significant number of atoms are displaced by less than 1 Å. The peak around 2.75 Å corresponds to oxygen atoms which have jumped to their nearest neighbor crystalline site. During the thermal spike a large number of atoms are displaced by less than 2 Å. The number of atoms which travel more than 2 Å is relatively constant up to ~5 Å. Therefore, applying a cut-off of 2 Å implies that the effect of the thermal vibrations even during the thermal spike is not taken into account.

Simulations presented in this article were performed on 64 nodes Dec-alpha parallel machine for over 100 000 time steps each. Due to computing time limits, only one simulation initiated with an energy of the PKA at 80 keV was performed and compared to a set of 28 cascades initiated with lower energies ranging from 5 keV to 20 keV.

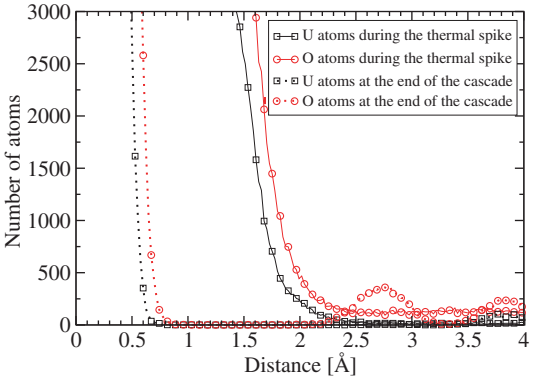


Fig. 1. Plot of the number of atoms as a function of the distance traveled starting from their initial position.

## 3. Results and discussion

### 3.1. Morphology of the cascade initiated at 80 keV

Fig. 2 shows snapshots of atoms displaced by more than 2 Å from their initial position during the displacement cascade. Within the first 60 femtoseconds (fs) a limited number of atoms are displaced. These atoms release their kinetic energy by binary collisions over several nanometers. In the following picosecond, atoms are seen to move large distances before undergoing another collision. However, once this occurs a new displacement cascade is initiated (called sub-cascade). Branches of these sub-cascades can be viewed in the two first snapshots at 0.1 ps and 0.15 ps. Half the kinetic energy of the PKA is released during this sequence known as the collision phase [9]. Subsequently (snapshot at 1.85 ps), the number of displaced atoms increases in each sub-cascade, while the average distance covered by the atoms drops significantly. No new sub-cascades are observed. This stage corresponds to the thermal spike and last until about 2 ps after the displacement start. Then during the following 2 ps many atoms return to their initial lattice

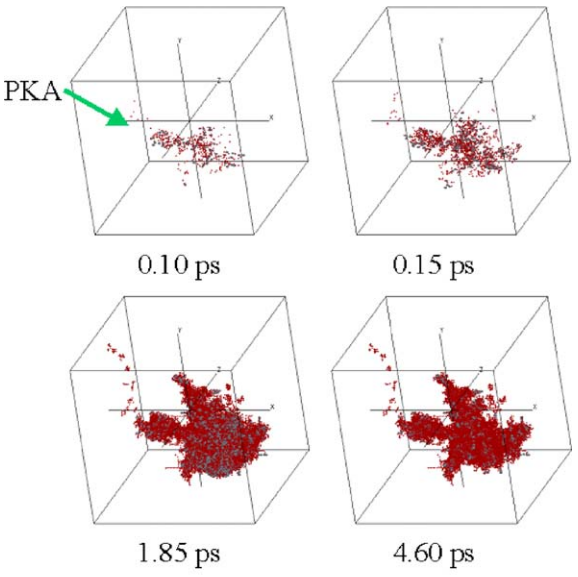


Fig. 2. Snapshots of the atoms displaced by more than 2 Å during the displacement cascade initiated at an energy of 80 keV. The arrow indicates the location and the orientation of the PKA.

position or to another crystalline site. This phase is called the restoration phase. In the snapshot at 4.60 ps less displaced atoms are observed than in the previous snapshot. At about 4 ps from the start of the cascade the structure remains stable, only few rearrangements take place. Finally, no amorphisation was found, 99.5% of the atoms return to the crystal lattice, and only few point defects are created.

At the end of the simulation five distinct sub-cascades have been counted. All sub-cascades range from ~5 nm to ~6 nm in size. This size corresponds approximately to the size of a cascade initiated with an energy of 20 keV [8]. Moreover, their centers of mass are each located at about 10 nm from the center of mass of the core of the cascade. On the periphery of the sub-cascades, numerous atom chains containing only oxygen or uranium atoms respectively are observed. These chains correspond to a linear collision sequence (LCS), where each atom collides with its first nearest neighbor of the same type along a particular direction. The last atoms of the linear collision sequence remains at an interstitial position. This observation is in agreement with the theory of Silsbee [20] and the pioneering MD work of Vineyard et al. [21] who proposed that the LCS's dominate the low energy development of displacement cascades. In $UO_2$ most of these LCS's take place in the $\langle 0\,0\,1\rangle$ direction. This is certainly due to the fact that the threshold displacement energy in this direction is the lowest.

### 3.2. Comparison with lower energy cascades

Although the size of the displacement cascade is larger than the cascades initiated with lower energy of the PKA, the main features of the cascade morphology are similar. Nevertheless, there are some quantitative differences.

The number of displaced atoms by more than 2 Å for different initial energies of the PKA are plotted in Fig. 3.

The plots show different behaviors as a function of the initial energies of the PKA. The number of displaced atoms increases steadily to 993 atoms for the cascade initiated at 5 keV, and to 4890 atoms for the cascade initiated at 20 keV. Only the cascade initiated at 80 keV shows a peak between 1 ps and 3 ps before reaching a total of 25 852 displaced atoms at the end of the cascade. As demonstrated in the Section 2 the cut-off distance of 2 Å does not take into account the effect of the thermal vibration even during the thermal spike. Moreover this distance is greater than half the distance between the first nearest neighbors for each type of atom: 3.86 Å and 2.73 Å for the U–U bonds and the O–O bonds respectively. Therefore, this peak corresponds to numerous atoms moving away from their initial lattice position, jumping to the next nearest neighbor site and finally returning into their original lattice position. The number of atoms involved in this phenomenon is approximately 25% of the total number of displaced atoms.

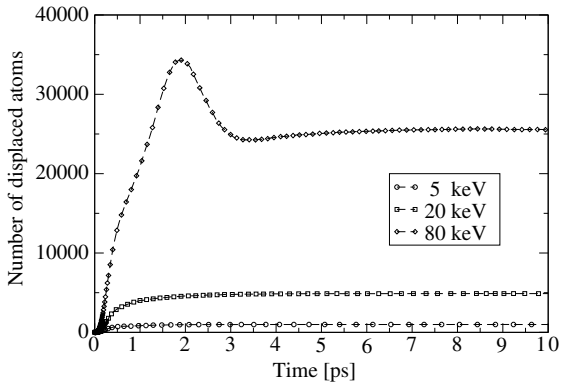


Fig. 3. Time evolution of the number of atoms displaced by more than 2 Å for cascades initiated with various energies of the PKA.

In order to explain this phenomenon we have studied closely the motion of the atoms in the core of the cascade. Fig. 4 depicts two slices of 5 Å width parallel to the (0 1 0) plan centered at the core of the cascade during the thermal spike at 2.15 ps (Fig. 4(a)), and at the end of the cascade at 20 ps (Fig. 4(b)).

Fig. 4(a) shows a zone of about 8 nm in diameter where the crystalline symmetry is destroyed exhibiting total disorder. This disorder imposes a local and temporary swelling which distorts the surrounding lattice. After 20 ps at the very end of the cascade (Fig. 4(b)), the lattice recovers its crystalline symmetry entirely and only a few point defects remain.

The track of this disorder can be viewed by comparing the total pair distribution functions during the thermal spike and at the end of the displacement cascade (Fig. 5). The amplitudes of the peaks during the thermal spike decrease and some peaks even disappear, indicating a loss of the crystalline order. This amorphisation is localized and its amplitude is smaller due to the surrounding lattice which remains unchanged.

To observe the local swelling we plotted the projection of the atomic positions in the (0 1 0) plan

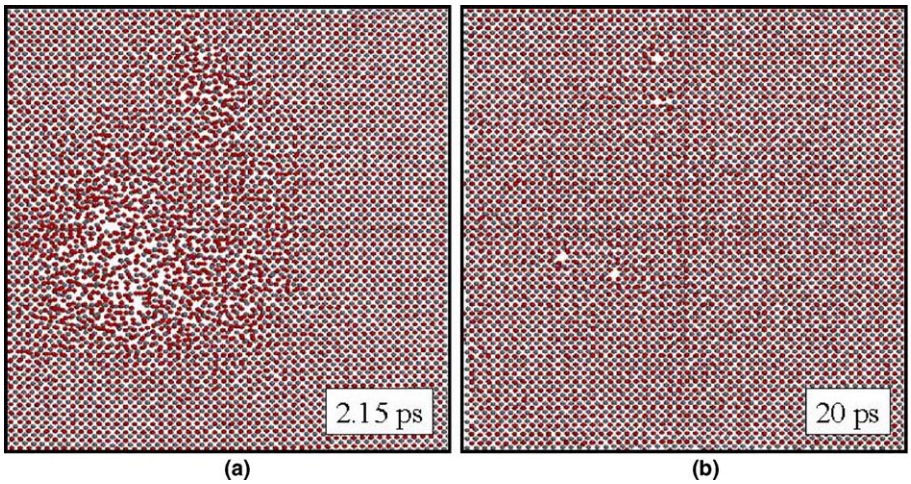


Fig. 4. Close up of the core of the displacement cascade at two different times: (a) at 2.15 ps corresponding to the end of the thermal spike and (b) at 20 ps corresponding to the very end of the cascade.

around the perturbed area during the thermal spike at 2.15 ps and at the end of the cascade at 20 ps in Fig. 6.

At 2.15 ps the lattice is bent by about 20 lattice plans with a maximum amplitude of 2.73 Å corresponding to the interatomic distance between two nearest oxygen neighbors. At 20 ps no distortion appears, the lattice network recovers its initial position. This phenomenon does not occur with such amplitude for cascades initiated with lower initial energy of the PKA. Such elastic distortion could lead to the formation of dislocations. One explanation for such phenomenon is that the kinetic energy transported here is significantly higher especially in the core of the cascade where interactions between sub-cascades occur.

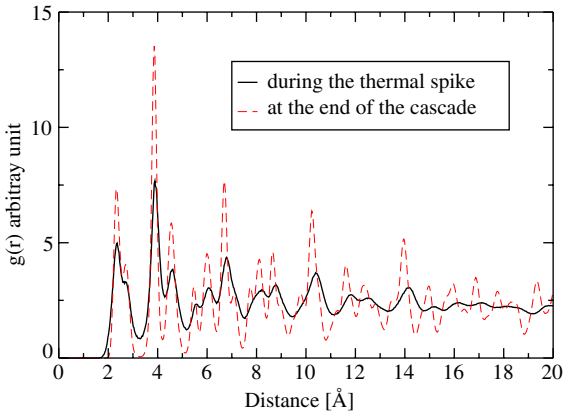


Fig. 5. Total pair distribution functions during the thermal spike (solid line) and at the end of the cascade (dashed line).

The number of atoms as a function of the distance traveled from their initial position is shown in Fig. 7(a) and (b) for the uranium and the oxygen atoms, respectively. The first peak around 2.7 Å in Fig. 7(a) corresponds to uranium atoms traveling to their nearest interstitial position. In the same figure, it can be seen that 75% of the uranium atoms displaced by more than 2 Å are on average only displaced up to their first nearest uranium neighbor. However, about 66% of the oxygen atoms, displaced by more than 2 Å, travel up to 5.4 Å which correspond to their fourth nearest oxygen neighbor. This indicate that oxygen atoms are able to travel larger distances and are therefore more mobile than uranium atoms.

Comparing the simulation carried out at 80 keV with the simulations carried out at lower initial energies, we found that the average distance traveled by uranium atoms displaced by more than 2 Å decreases from 5.35 Å to 4.58 Å as the initial energy of the PKA increases. More displaced uranium atoms move only up to their first nearest neighbor. This indicates that the number of linear collision sequences is more important at higher energy cascades. However, for the oxygen atoms the trend is reverse. The distance traveled increases from 3.88 Å (corresponding to the second nearest neighbor) to 4.45 Å (corresponding to the third nearest neighbor) as the energy of the initial PKA increases. This means that the recombination takes place over larger length scales when the cascade energy increases. Nevertheless, for all the simulation cascades and almost all the atoms the distance

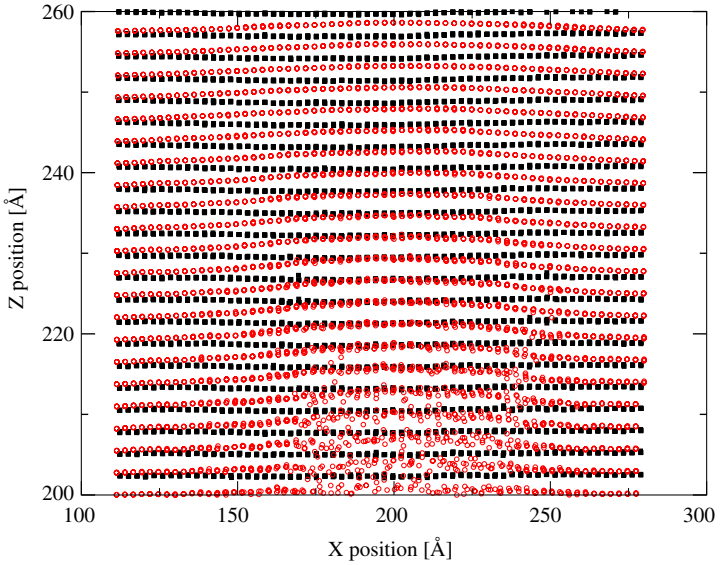


Fig. 6. Projection of the atomic positions in the (0 1 0) plan around the perturbed zone at 2.15 ps (○) and 20 ps (■).

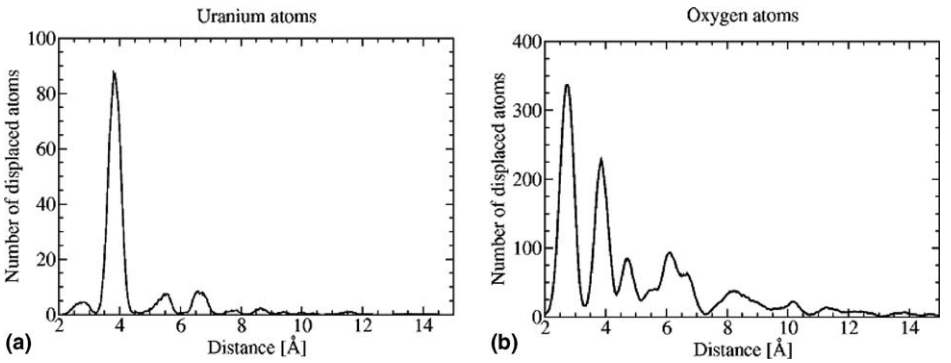


Fig. 7. Plots of the number of displaced atoms by more than 2 Å as a function of the distance covered at the end of the displacement cascade initiated at an energy of 80 keV: (a) uranium atoms; (b) oxygen atoms.

traveled does not exceed 15 Å at the end of the simulation.

### 3.3. Point defects study

The study of the primary damage state requires the quantification of the number of point defects created and their localization in the matrix as well as the understanding of the number of displaced atoms which could be related to the number of displacement per atom number (dpa). The number of atoms displaced by more than 2 Å and the number of interstitials during the displacement cascade initiated at 80 keV are shown in Fig. 8.

An atom is counted in an interstitial position if it is located in a sphere of radius 2.8 Å centered on the ideal interstitial position in the perfect lattice. After 2 ps the number of uranium interstitials and the number of oxygen interstitials drop dramatically. Within approximately 3 ps only few interstitials remain, indicating that the structure has almost entirely recovered. The lifetime of the cascade is estimated when the number of the displaced atoms remains stable. For the cascade initiated at 80 keV its lifetime is about 5 ps, which is smaller than the 9 ps estimated by the theory [2]. The difference stems from the fact that the cascade is more compact than estimated by the theory. Thus, an atom undergoes more collisions during the simulations, and the energy is then dissipated faster.

At the end of the cascade few point defects have been created: 134 for the uranium atoms and 270 for

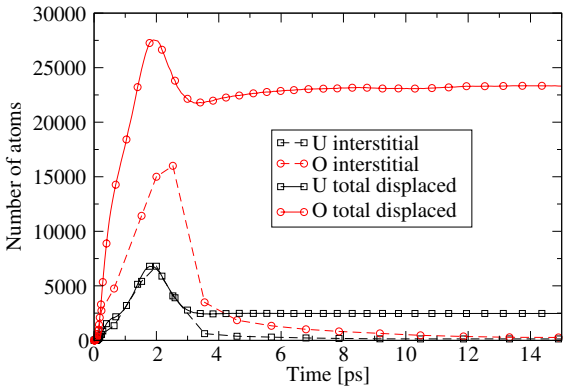


Fig. 8. Plots of the number of atoms displaced by more than 2 Å and the number of interstitial created during the displacement cascade initiated with an energy of 80 keV.

the oxygen atoms; but a total of 25 852 atoms have been displaced. These quantities are in agreement with the values estimated previously with simulations initiated at smaller PKA energies [8]. Proportionally, 90.5% of the displaced atoms are oxygen atoms. This confirms that oxygen atoms are more mobile than the uranium atoms. The uranium atoms are harder to move because of their higher mass and higher threshold displacement energy. The relatively limited number of displaced uranium atoms and the high mobility of the oxygen atoms promote the recovery of the crystalline lattice. Furthermore, at the end of the displacement cascade, 5.4% of the displaced uranium atoms remain in an interstitial position while only 1.2% of the displaced oxygen atoms are found in such position. Because an irrelevant number of dumbbells and no antisite have been found, the difference between the number of interstitials and the number of displaced atoms at the end of the cascade corresponds to replacement atoms. Therefore, more oxygen atoms are involved in the replacement sequences.

Comparing these results with those obtained for smaller PKA energies, the ratio of the displaced atoms per chemical species remains approximately constant as the initial PKA energy increases. About 90% of the total displaced atoms are oxygen atoms and 10% only are uranium atoms. On the contrary, the ratio of the number of uranium interstitials at the end of the cascade versus the number of displaced uranium atoms drops significantly from 22% for a cascade initiated with an energy of 5 keV to about 13% for 20 keV and to 5.4% for 80 keV. We note that this ratio remains constant for the oxygen atoms. With the increase of the initial PKA energy, the number of displaced uranium atoms increases due to a higher temperature in the core of the cascade and more collision sequences.

Usually, the creation of an interstitial leads to the creation of a vacancy, which produces a Frenkel pair. The evolution of the number of the Frenkel pairs versus the initial PKA energy observed in our simulations and calculated using the NRT (Norton–Robinson–Torrens) law are compared in Fig. 9. Each points in Fig. 9, excepted the ones at 80 keV, correspond to an average value over 7 different cascade simulations. The theoretical linear NRT law [22,23] usually used to count the number of point defects created as a function of the energy is defined as follows:

$$N_{\mathrm{NRT}} = \frac{0.8E}{2E_{\mathrm{d}}}, \tag{1}$$

where $E_{\mathrm{d}}$ is the average value of the threshold displacement energy (herein 30 eV).

The evolutions of the number of Frenkel pairs with the initial energy of the PKA can be fitted to a power law $N_{\mathrm{f}} \propto E^{\mathrm{n}}$ with an exponent equal to 0.86 for the uranium atoms and to 0.84 for the oxygen atoms. At the end of the cascade the number of Frenkel pairs created is half the number estimated by the NRT law. This discrepancy has been already found in MD simulations of several materials: Cu [24], Fe [25], $Ni_3Al$ [26], Ti and Zr [27]. The difference probably stems from the fact that the NRT law does not take into account the recombinations during the annealing process and the thermal spike.

For both high and low initial energies of the PKA, the spatial distributions of the point defects are not homogeneous. The interstitial atoms are

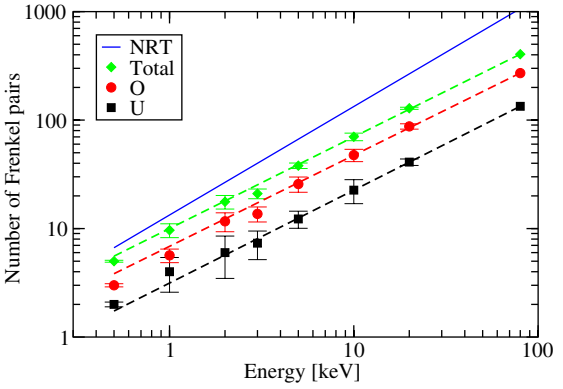


Fig. 9. Log–log plots of the total number of Frenkel pairs and of the total of Frenkel pair per atom type versus the initial PKA energy. Our results are compared with the theoretical plot of the NRT law.

located at the periphery of the branches of the sub-cascades while the vacancies are mainly found in the core of each sub-cascades.

## 4. Conclusion

For the first time a displacement cascade has been initiated with a realistic energy of the recoil nucleus using classical molecular dynamics simulation. This cascade involves the displacement of a total of 25852 atoms but only 404 point defects are created at the end of the cascade. This simulation confirms the previously estimated values for the Frenkel pairs creation as well as the discrepancy found with the theoretical NRT law [8]. The main morphology features of this displacement cascade are the same than those found for cascades initiated with lower PKA energies: creation of sub-cascade branches and creation of few point defects but no amorphisation. These point defects are also preferentially localized; the interstitials are localized at the periphery of the sub-cascade branches, and the vacancies in the core of each sub-cascades. The main sub-cascades are separated by about 10 nm and their size is in the same order of magnitude as the cascade initiated with an initial PKA energy of 20 keV. As a consequence, the main physical phenomena occurring in $UO_2$ displacement cascades can adequately be described with a small initial PKA energy.

However, the lifetime and the size of the high energy cascade are larger and some of the statistics are different. Partial and temporary amorphisation of the matrix over a large length scale was only found in such cascade leading to an amplification of the elastic distortion during the thermal spike that could lead to further damage such as dislocations. Proportionally in the high energy cascade, the uranium atoms undergo more linear collision sequence and oxygen atoms recombine over a longer distance as the energy of the cascade increases.

In all the cases the uranium sublattice undergoes few damage and the oxygen atoms exhibit has a great mobility. Consequently, the reconstruction of the crystal fluorite lattice is fast and does not lead to any amorphisation at the end of the cascade.

## References

[1] W.J. Weber, Radiat. Eff. 83 (1984) 145.
[2] R.T. Robinson, J. Nucl. Mater. 216 (1994) 1.
[3] D.J. Bacon, T. Diaz de la Rubia, J. Nucl. Mater. 216 (1994) 275.
[4] F. Gao, W.J. Weber, R. Devanathan, Nucl. Instrum. and Meth. B 180 (2001) 176.
[5] L. Veiller, J.P. Crocombette, D. Ghaleb, J. Nucl. Mater. 306 (2002) 61.
[6] A. Abbas, J.M. Delaye, D. Ghaleb, G. Calas, J. Non-Cryst. Solids 315 (2003) 187.
[7] J.M. Delaye, D. Ghaleb, Phys. Rev. B 135 (1998) 201.
[8] L. Van Brutzel, J.-M. Delaye, D. Ghaleb, M. Rarivomanantsoa, Philos. Mag. 83 (2003) 4083.
[9] R.S. Averback, D.N. Seidman, Mater. Sci. Forum 15–18 (1987) 963.
[10] N. Nakae, Y. Iwata, T. Kirihara, J. Nucl. Mater. 80 (1979) 314.
[11] Hj. Matzke, Nucl. Instrum. and Meth. B 65 (1992) 30.
[12] Hj. Matzke, L.M. Wang, J. Nucl. Mater. 231 (1996) 155.
[13] W.J. Weber, J. Nucl. Mater. 98 (1981) 206.
[14] N.D. Morelon, D. Ghaleb, L. Van Brutzel, Philos. Mag. 83 (2003) 1533.
[15] C.S. Becquart, C. Domain, A. Legris, J.C. Van Duysen, J. Nucl. Mater. 280 (2000) 73.
[16] J.P. Crocombette, F. Jollet, L. Thien Nga, T. Petit, Phys. Rev. B 64 (2001) 104.
[17] Hj. Matzke, J. Chem. Soc., Faraday Trans. II 83 (1987) 1121.
[18] J.W. De Leeuw, E.R. Smith, Proc. R. Soc. A 27 (1980) 373.
[19] J.F. Ziegler, J.P. Biersack, U. Littmark, The Stopping Range of Ions in Matter, Pergamon, Oxford, 1985.
[20] R.H. Silsbee, J. Appl. Phys. 28 (1957) 1246.
[21] J.B. Gibson, A.N. Goland, M. Milgram, G.H. Vineyard, Phys. Rev. 120 (1960) 458.
[22] M.T. Robinson, I.M. Torrens, Phys. Rev. B 9 (1972) 5008.
[23] I.M. Torrens, M.T. Robinson, in: J.W. Corbett, L.C. Ianniello (Eds.), Radiation-induced Voids in Metals, US Atomic Energy Commission, Washington, DC, 1972, p. 739.
[24] T. Diaz de la Rubia, M.W. Guinan, Mater. Res. Forum 97–99 (1992) 23.
[25] R.E. Stoller, Microstructure of irradiated materials, in: I. Roberston, L. Rehn, S. Zinkle, W. Phythian (Eds.), Materials Research Society Symposium Proceeding, vol. 373, Material Research Society, Pittsburgh, Pennsylvania, 1995, p. 21.
[26] J.C. Turbatte, J. Ruste, Internal report EDF, HT-41/96-019/A.
[27] F. Gao, D.J. Bacon, Philos. Mag. A 71 (1995) 43.